Photoelectron imaging of 8p Rydberg states of atomic iodine following methyl iodide A-band decomposition

ARTICLE *in* JOURNAL OF MOLECULAR SPECTROSCOPY · SEPTEMBER 2009

Impact Factor: 1.48 · DOI: 10.1016/j.jms.2009.08.003

4 AUTHORS, INCLUDING:

Linqiang Hua
Chinese Academy of Sciences
9 PUBLICATIONS **42** CITATIONS
SEE PROFILE

Changjin Hu
Chinese Academy of Sciences
27 PUBLICATIONS **154** CITATIONS
SEE PROFILE

Bing Zhang
University of Nevada, Las Vegas
225 PUBLICATIONS **2,590** CITATIONS
SEE PROFILE

Journal of Molecular Spectroscopy 257 (2009) 200–204

Contents lists available at ScienceDirect

Journal of Molecular Spectroscopy

journal homepage: www.elsevier.com/locate/jms

Photoelectron imaging of 8p Rydberg states of atomic iodine following methyl iodide A-band decomposition

Huan Shen, Linqiang Hua, Changjin Hu, Bing Zhang *

State Key Laboratory of Magnetic Resonance and Atomic and Molecular Physics, Wuhan Institute of Physics and Mathematics, Chinese Academy of Sciences, Wuhan 430071, PR China
Graduate School of the Chinese Academy of Sciences, Beijing 10036, PR China

ARTICLE INFO

Article history:
Received 25 May 2009
In revised form 15 July 2009
Available online 12 August 2009

Keywords:
Photoelectron imaging
Iodine atom
Intermediate state
Final ion levels

ABSTRACT

Photoelectron imaging technique has been applied to study (2 + 1) REMPI of atomic iodine through 8p Rydberg states around 253 nm. Full three-dimensional state-specific speed and angular distributions of the photoelectrons were recorded. The branching ratios among the different I^+ levels revealed that the perturbation on $(^3P_2)8p$ series is particularly large among the $(^3P_2)np$ series. The violation of core-conserving ionization is attributed to the interactions between the $(^3P_2)8p$ and $(^1D_2)6p$ series. The photoelectron angular distributions were found to be well characterized by $P_2(\cos\theta)$ and $P_4(\cos\theta)$. A relatively high positive β_2 and a relatively low β_4 observed in (2 + 1) REMPI process indicated that the ionization process can be approximately considered as single-photon ionization via the weakly aligned $(^3P_2)8p$ intermediate states.

1. Introduction

The A-band photolysis of CH_3I in the ultraviolet region of the spectrum (220–350 nm) is an important benchmark for studying the photodissociation of small polyatomic molecules for both practical and fundamental reasons [1]. It is well accepted that the photodissociation process of CH_3I serves as a prototype for understanding dissociation of the molecules with C_{3v} symmetry [2] and even for deep insight into the dissociation mechanism of long chain halide molecules [3,4]. Furthermore, A-band photodissociation of CH_3I can be treated as a good source of study on spectroscopy for both iodine atom and methyl radical. And many works have been carried out by taking this advantage and much valuable information has been obtained [5–9]. Among the $5p^4nl$ Rydberg series of I atom, $5p^4np$ Rydberg series have attracted much attention and were frequently studied. One important study in the early time was carried by Minnhagen [5]. In the study, numerous energy levels of $5p^4nl$ series were assigned and it was found that the perturbation on $5p^4(^3P_2)np$ series is particularly large for $n = 8$. Later on, Pratt also identified many Rydberg states of iodine using photoelectron spectroscopy [6] and multiphoton ionization (MPI) spectrum [7]. Following the application of velocity map imaging technique [10], directly and simultaneously measuring the velocity and angular distributions of photoions (or photoelectrons [11]) with high resolution becomes practicable. By taking the advantage of the photoelectron imaging, Jung and co-workers studied $5p^46p$, $5p^47p$, $5p^48p$ and $5p^44f$ Rydberg series of atomic iodine among the wavelength region of 277–313 nm via (2 + 1) resonance-enhanced multiphoton ionization (REMPI) scheme [8]. They found that the final ion level distributions are generally dominated by the core-level conserving propensity of resonant excited-state. Another study carried out lately by Hu et al. has investigated (2 + 1) REMPI of ground state atomic iodine via $5p^4(^1D_2)6p$ and $5p^4(^3P_2)4f$ Rydberg states over the wavelength range of 245.5–261.5 nm [9]. In this study, the similar core-level conserving propensity of resonant excited-state was found for the final ion state distributions of $(^1D_2)6p$ Rydberg series, while for $(^3P_2)4f$ intermediate states, some observable deviation from this simple picture was reported.

In the present study, we report the photoionization on the $(^3P_2)8p$ Rydberg states of atomic iodine around 253 nm using photoelectron imaging technique. Although three states among the 8p Rydberg series have been reported by Jung et al. [8], others remain unstudied and a comprehensive study is needed. Besides, the perturbations on $5p^4(^3P_2)np$ series have been reported to be particularly large for $n = 8$ [5], and thus, interesting information is expected when a new technique is employed.

2. Experimental section

The photoelectron imaging setup used in this study has been described elsewhere [12] and is based upon the application of velocity map imaging method [10]. Briefly, a pulsed molecular beam is produced by expending a gas mixture (approximated 5% CH_3I in helium) into the source chamber via a general valve with a 0.6-mm-diameter orifice. After passing through a skimmer,

* Corresponding author. Fax: +86 27 87198576.
E-mail address: bzhang@wipm.ac.cn (B. Zhang).

0022-2852/$ - see front matter © 2009 Elsevier Inc. All rights reserved.
doi:10.1016/j.jms.2009.08.003

which separate the source chamber from the ionization chamber, the molecular beam is intersected at right angles by a laser beam generated by an Nd:YAG pumped dye laser. Only one laser beam is employed in this study, and thus the same laser is used both for the A-band photodissociation of CH_3I and subsequent resonant ionization of the neutral iodine atom photofragments. The laser is vertically polarized (parallel to the plane of the two-dimensional detector) and is focused using a lens with a 25 cm focal length. The ground state of iodine atom photofragments was ionized using (2 + 1) REMPI. The photoelectrons produced are extracted and accelerated by the electrostatic immersion lens into the TOF (time of flight) tube, and impinge into a 2D (two-dimensional) position-sensitive detector at last. 2D photoelectron images on the phosphor screen are recorded using a charge coupled device (CCD) camera, and accumulated over 20 000 laser shots with the background removed by subtraction of a reference image collected at off-resonance wavelength under the same conditions. In order to minimize the effect of the earth's magnetic field on the photoelectron trajectory, a double-layer μ-metal shield was installed along the axis of the whole ionization chamber.

3. Results and discussion

3.1. Photoelectron images and relative branching ratios among final ion levels

The raw photoelectron images resulted from REMPI of the iodine atom fragments following the A-band photolysis of CH_3I at four different wavelengths are displayed in Fig. 1. According to the earlier investigations [5], the nascent iodine atom can be assigned as $5p^5\ ^2P_{3/2}$ at these wavelengths and the assignments of the intermediate states (2 + 1) of REMPI process are given in Table 1. These raw images are the two-dimensional projections of three-dimensional speed and angular distributions of the photoelectrons.

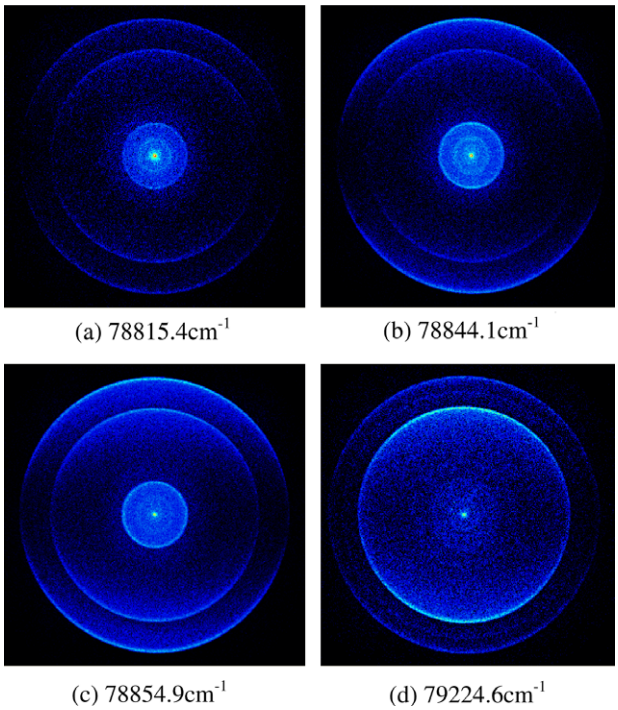

Fig. 1. Raw two-dimensional images of the photoelectrons ejected from the $I(^2P_{3/2})$ fragment via (2 + 1) REMPI at different $2h\nu$ energy. (a) 78815.4 cm^{-1}, (b) 78844.1 cm^{-1}, (c) 78854.9 cm^{-1} and (d) 79224.6 cm^{-1}. The laser polarization vectors are parallel to the vertical axis.

Table 1
Product relative branching ratios among final ion levels result from the (2 + 1) REMPI processes of the fragment $I(^2P_{3/2})$ atom.

$2h\nu$ energy/cm^{-1}	Intermediate state	Branching ratio (%)		
		$I^+(^1D)$	$I^+(^3P_{0,1})$	$I^+(^3P_2)$
78815.4	$(^3P_2)8p[2]_{3/2}$	36.17	10.02	53.81
78844.1	$(^3P_2)8p[3]_{7/2}$	15.88	6.43	77.69
78854.9	$(^3P_2)8p[3]_{5/2}$	29.38	4.71	65.91
		26[a]	4[a]	70[a]
79224.6	$(^3P_2)8p[1]_{3/2}$	66.59	6.71	26.70

[a] Results form Ref. [8].

Given the fact that the original distribution has cylindrical symmetry around the polarization axis of the photolysis laser, a full three-dimensional photoelectron image could be reconstructed by using the basis-set expansion method (BASEX) [13]. Thus, the speed distribution of photoelectrons $P(\upsilon_{e^-})$ is obtained from the angle integration of the reconstructed image as a function of the radial distance from the center, as shown in Fig. 2.

The speed of photoelectron can be derived from the energy conservation relationship,

$$\upsilon_{e^-} = \sqrt{\frac{2(3h\nu + E_0 - E_i)}{m_{e^-}(m_{e^-} + m_i)/m_i}} \quad (1)$$

Where $h\nu$ is the photon energy, E_0 the internal energy of photofragment iodine atom with respect to the ground state $I(^2P_{3/2})$, E_i the internal energy of ionic iodine at the ith level, and m_{e^-} (m_i) the mass of the electron (ion). The speed distribution of photoelectrons was range from 0 to 1300 km s^{-1}, which corresponding to the different ion levels of iodine and methyl iodine. The slow-speed features with the speed less than 350 km s^{-1}, which are out of our focus in this report, were considered to be originated from the two-photon ionizations of the parent molecule CH_3I [14], while the other speed peaks can be assigned to the final iodine ion levels from (2 + 1) REMPI of the ground state of atomic iodine. If an outer electron was removed away from atomic iodine, the configuration for I^+ is $[Kr]5s^25p^4$, which yields five levels above the ground state of ionic iodine [5,15]. They are $^3P_2$, $^3P_0$, $^3P_1$, $^1D_2$, and $^1S_0$ at 84295.1, 90743.0, 91382.1, 98022.3, and 113796.4 cm^{-1}, respectively. With these energy levels, the dominant peaks in the $P(\upsilon_{e^-})$ distributions can be assigned to the final iodine ion levels as shown in Fig. 2.

The present study is concerned with two-photon transitions from the ground state of atomic iodine to the $(^3P_2)8p$ Rydberg states, and subsequently ionized by one photon. We depict the (2 + 1) REMPI process for I atom as follows:

$$I(^{2s+1}L_J) \xrightarrow{2h\nu} I^*((^{2s_c^{+1}}L_{J_c})nl[K]_J) \xrightarrow{h\nu} I^+(^{2s^+ + 1}L_{J^+}^+) + e^-(KE) \quad (2)$$

The symbols of "∗"and "+" denote the intermediate resonant state and the final ion state, respectively. The initial and finial levels are labeled using the LS coupling scheme, while the intermediate excited states of neutral iodine are described as $J_c l$ coupling according to the Minnhagen's work [5]. In the $J_c l$ coupling scheme, the spin–orbit interaction of the outer electron is considered to be smaller than the electrostatic interaction of this electron with $[Kr]5s^25p^4$ core [5]. That is, the spin–orbit interaction of outer electron could be neglected, only the electrostatic interaction was considered in the present intermediate configuration. In this coupling scheme, the total angular momentum of the ion core, J_c, is coupled to the orbital angular momentum of the outer electron, l, to given K. The spin of the Rydberg electron, s, is then coupled to K to given the total angular momentum, J'. In this work, the intermediate states are then labeled as $(^3P_2)8p[K]_{J'}$, where $(^3P_2)$ describes the ion core.

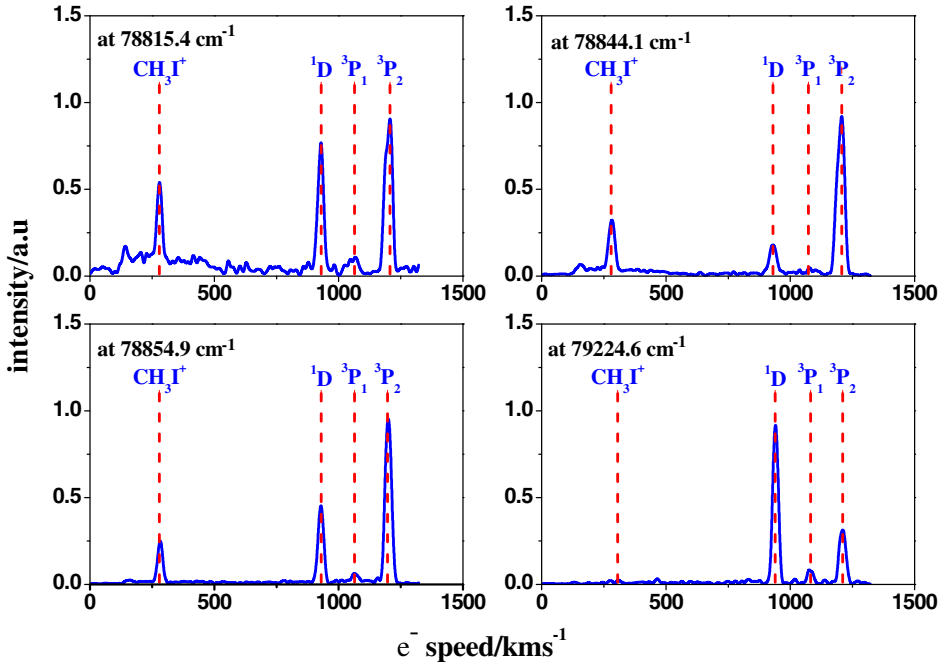

Fig. 2. The speed distributions of photoelectron obtained from the images shown in Fig. 1. The assignments of the final ion levels are indicated.

The two-photon absorptions from the $5p^5\ ^2P_{3/2}$ states of the iodine atom and the relative branching ratios among final ion levels are calculated and summarized in Table 1. Previously, core-preserving ionization has been clearly demonstrated in REMPI process in which Rydberg electron is removed from the resonant Rydberg state without relaxation of the ionic core [16]. In other words, the formation of ionic levels from a (2 + 1) REMPI process will depend on the electronic configuration of the resonant intermediate state. In the present study, three intermediate levels, $(^3P_2)8p[2]_{3/2}$, $(^3P_2)8p[3]_{7/2}$ and $(^3P_2)8p[3]_{5/2}$ were found to be consistent with this regulation well since the ratio which converged to $^3P_2$ core is over 50% (see Table 1), which means that the core-level conserving propensity play a key role in accounting for the final ion distribution in these cases. Previous work has also demonstrated core-preserving ionization in rare gas atom [16]. However, the success of core-preserving ionization apparently depends on the absence of strong perturbation of the resonant state by other configurations having different ion cores and the avoidance of complicating autoionization structure in the continuum. In reality, the relatively high $I^+(^1D_2)$ branching ratio and some population in $I^+(^3P_{0,1})$ were also found in these $(^3P_2)8p$ Rydberg series, which indicate considerable deviation from the simple core-conserving picture.

The violation of core-conserving ionization is attributed to several factors including the autoionization resonance in the ionization continuum and the configuration interaction of the resonance state with the other excited states with different ion cores [8]. However, a nearly identical relative branching ratio was observed by Jung et al. [8] and the present work for $(^3P_2)8p[3]_{5/2}$ intermediate state (see Table 1). Although both studies invoke the same experimental method and the same intermediate resonant state, the initial states are different and so the total ionization energies. Thus, the identical branching fractions among final ion states from the two studies provide a strong support for the negligible autoionization effects. It seems that the configuration interaction among the resonance states play a key role in the deviation from core-conserving ionization. Generally, configuration interaction can occur in the high lying states when the J' numbers and the parity of both states are the same. And the interaction will become stronger as the energy difference between mixing states goes smaller [17]. The energy level for $(^3P_2)8p$ and $(^1D_2)6p$ series of I atom are around 79 000 cm^{-1}, and the difference between the states with the same K and J' are within a few hundred wave numbers [5]. That probably explained why the interaction between these two series is particularly strong, which is consistent with the previous studies where the perturbation $(^3P_2)8p$ series of I atom by $(^1D_2)6p$ series was reported [5]. If the two interacting configurations involve different ion cores, the perturbation can be revealed in the branching ratio of the final ion states. In this work, this perturbation is confirmed quantitatively. The branching ratio for ions with $^1D_2$ core is obviously high, 36.17% for $(^3P_2)8p[2]_{3/2}$ and even high to 66.59% for $(^3P_2)8p[1]_{3/2}$.

A further comparison can also be made for $(^3P_2)6p$, $(^3P_2)7p$ and $(^3P_2)8p$ series, as shown in Table 2. The deviation in 8p series is the largest, which well agrees with Minnhagen's conclusion [5]. Generally, for a given l the series with the highest J' should be least perturbed [5]. In Table 2, we found that the trend of $^3P_2$ branching ratio for $(^3P_2)6p$ and $(^3P_2)7p$ series were consistent with this regulation very well, which has the lowest $^3P_2$ branching ratio for $[1]_{1/2}$ states, and the highest for $[3]_{7/2}$ states. As to $(^3P_2)8p$ series, the regulation also seems to be applicable although $^3P_2$ branching ratio for $[2]_{5/2}$ state was found to be a little higher than expected. It is worth pointing out that $(^1D_2)6p$ series can be well described by the core-level conserving propensity. From the results obtained by Jung et al. [8] and Hu et al. [9], the $^1D_2$ branching ratios for $(^1D_2)6p$ series were found to be very large indeed and all of them exceed 85%, even up to 100%. Obviously, the perturbation between $(^3P_2)8p$ and $(^1D_2)6p$ series has different influence on each side.

Table 2
$^3P_2$ branching ratios (%) for different intermediate states of $(^3P_2)6p$, $(^3P_2)7p$ and $(^3P_2)8p$ series.

	$[1]_{1/2}$	$[1]_{3/2}$	$[2]_{3/2}$	$[2]_{5/2}$	$[3]_{5/2}$	$[3]_{7/2}$
6p	75[a]	82[a]	93[a]	98[a]	96[a]	100[a]
7p	80[a]	80[a]			97[a]	
8p	46[a]			90[a]	70[a]	
		26.70[b]	53.81[b]		65.91[b]	77.69[b]

[a] Results form Ref. [8].
[b] Results obtained in this study.

More experimental and theoretical works will be needed for deeper understandings of this difference.

3.2. Angular distribution of ejected photoelectrons

The photoelectron angular distributions using linear polarized light were determined. For linear polarization, the electron intensity was obtained as a function of angle between the laser polarization axis and the momentum vector of the emitted photoelectrons. Basing on the reconstructed images inverted by the BASEX method [13], the level-selective photoelectron angular distribution, $I(\theta)$, can also be obtained by integrating the reconstructed three-dimensional speed distribution over a proper range of speed at each angle. Generally, angular distribution of photoelectrons emitted by $(n + 1)$ REMPI with linearly polarized radiation can be expressed by the following relationship:

$$I(\theta) \propto \sum_{k=0}^{k_{max}} \beta_{2k} P_{2k}(\cos\theta) \quad (3)$$

Where $k_{max} = n + 1$ for a $(n + 1)$ REMPI process, $P_{2k}(\cos\theta)$ are the Legendre polynomials of degree $2k$, and β_{2k} are the anisotropy coefficients [18,19]. All of our angular distributions are found to be quite fit with $k_{max} = 2$, as listed in Table 3. Three typical angular distributions and fitted results are also displayed as polar plots in Fig. 3.

For an $(n + 1)$ REMPI process in which only one intermediate J'-level is populated, the k_{max} will be constrained by the smaller of $n + 1$, $J' + 1$, or l_{max}. Here l_{max} is the maximum orbital angular momentum component of the ejected photoelectrons [19,20]. The sum $J' + 1$ (or $n + 1$) gives the total anisotropy created in the final state from J'(or n) angular momentum in the intermediate state and one unit of angular momentum from the ionization photon. l_{max} reflects the maximum anisotropy the photoelectron can exhibit. In the direct one-electron ionization, the character of outgoing electrons from $(^3P_2)8p$ states is a mixture of s and d partial waves due to the parity rule $\Delta l = \pm 1$ and l_{max} then equal to 2. Hence, k_{max} is likely limited by l_{max}. Our analytical fit shows that the photoelectron angular distributions are well characterized by $P_2(\cos\theta)$ and $P_4(\cos\theta)$ for all transitions. The constraint $k_{max} = l_{max}$ also gives the close connection between the photoionization dynamics of the final step and the observed photoelectron angular distribution. In this regard, $(n + 1)$ REMPI angular distributions can provide very much the same information as in the conventional one-photon photoelectron angular distribution.

In single-photon ionization, the photoelectron angular distribution can be expressed by the first order term with Eq. (3). The β_2 coefficient reflects the angular distribution resulting from the single-photon ionization of an isotropic intermediate state. On the other hand, the higher order terms in Eq. (3) reflect the alignment of the total angular momentum of the intermediate states. The photoelectron angular distributions obtained for $(2 + 1)$ REMPI through the $(^3P_2)8p$ states are characterized by a relatively high positive β_2 and a relatively low β_4. The high positive β_2 suggests that $(2 + 1)$ REMPI of atomic iodine can be considered as single-photon ionization of a highly excited-state, while the low β_4 reflects the weak effect of the alignment in the $(^3P_2)8p$ intermediate states.

Table 3
Legendre weighting coefficients β_{2k} of photoelectron angular for the $(2 + 1)$ REMPI processes of the ground state $I(^2P_{3/2})$.

Intermediate State	$I^+(^1D)$		$I^+(^3P_{0,1})$		$I^+(^3P_2)$	
	β_2	β_4	β_2	β_4	β_2	β_4
$(^3P_2)8p[2]_{3/2}$	0.99	0.06	0.81	0.21	1.48	0.05
$(^3P_2)8p[3]_{7/2}$	1.12	0.17	0.92	0.10	1.89	0.22
$(^3P_2)8p[3]_{5/2}$	1.36	0.05	0.88	0.18	1.68	0.09
$(^3P_2)8p[1]_{3/2}$	1.12	0.05	0.86	0.04	1.38	0.05

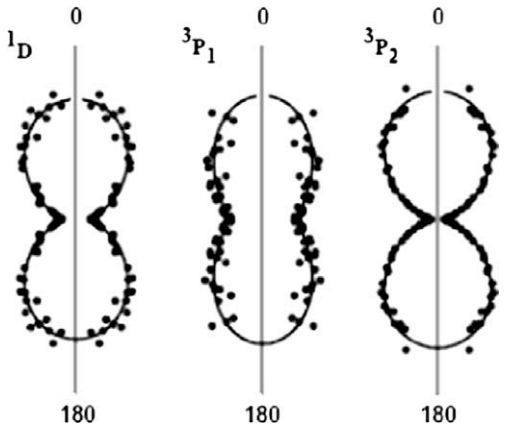

Fig. 3. Three representative photoelectron angular distributions were shown in the polar diagrams. The laser polarization is vertical. The dots are the experimental results for the final ion states $I^+(^1D)$, $I^+(^3P_1)$ and $I^+(^3P_2)$, at 78854.9 cm^{-1}. The solid lines are the corresponding fits using Eq. (3).

4. Conclusion

We have investigated the photoionization dynamics of the iodine atom using photoelectron imaging technique coupled with $(2 + 1)$ resonance-enhanced multiphoton ionization. The intermediate levels which converge to the $(^3P_2)8p$ levels were studied via the ground state of atomic iodine $5p^5\ ^2P_{3/2}$. The relative branching ratios of the final ion levels revealed that the perturbation on $(^3P_2)8p$ series were particularly large among the $(^3P_2)np$ series. Significant deviations from the simple core-conserving picture were observed and attributed to the interactions between $(^3P_2)8p$ and $(^1D_2)6p$ configurations. The angular distributions of outgoing photoelectrons were also obtained, and found to be well characterized by $P_2(\cos\theta)$ and $P_4(\cos\theta)$, namely $k_{max} = 2$, for all transitions. The high positive β_2 indicated that the ionization process of $(2 + 1)$ REMPI can be approximately considered as single-photon ionization, while the low β_4 reflects the weak effect of the alignment in the $(^3P_2)8p$ intermediate states.

Acknowledgments

All the authors gratefully acknowledge support from the National Science Foundation of China under Grant No. 20703060.

References

[1] R.K. Sparks, K. Shobatake, L.R. Carlson, Y.T. Lee, J. Chem. Phys. 75 (1981) 3838.
[2] M.N.R. Ashfold, N.H. Nahler, A.J. Orr-Ewing, O.P.J. Vieuxmaire, R.L. Toomes, T.N. Kitsopoulos, I.A. Garcia, D.A. Chestakov, S.M. Wu, D.H. Parker, Phys. Chem. Chem. Phys. 8 (2006) 26.
[3] Y. Wang, S. Zhang, Z. Wei, Q. Zheng, B. Zhang, J. Chem. Phys. 125 (2006) 184307.
[4] Y. Tang, W.B. Lee, Z. Hu, B. Zhang, K.C. Lin, J. Chem. Phys. 126 (2007) 064302.
[5] L. Minnhagen, Ark. Fys. 21 (1962) 415.
[6] S.T. Pratt, Phys. Rev. A 33 (1986) 1718.
[7] S.T. Pratt, P.M. Dehmer, J.L. Dehmer, Chem. Phys. Lett. 126 (1986) 12.
[8] Y.J. Jung, Y.S. Kim, W.K. Kang, K.H. Jung, J. Chem. Phys. 107 (1997) 7187.
[9] C. Hu, S. Pei, Y.L. Chen, K. Liu, J. Phys. Chem. A 111 (2007) 6813.
[10] A.T.J.B. Eppink, D.H. Parker, Rev. Sci. Instrum. 68 (1997) 3477.
[11] H. Helm, N. Bijerre, M.J. Dyer, D.L. Huestis, M. Saeed, Phys. Rev. Lett. 70 (1993) 3221.
[12] L. Hua, H. Shen, C. Hu, B. Zhang, J. Chem. Phys. 129 (2008) 244308.
[13] V. Dribinski, A. Ossadtchi, V.A. Mandelshtam, H. Reisler, Rev. Sci. Instrum. 73 (2002) 2634.
[14] C. Hu, S. Pei, C. Chang, K. Liu, Mol. Phys. 106 (2008) 405.

[15] R.E. Huffman, J.C. Larrabee, Y. Tanaka, J. Chem. Phys. 47 (1967) 856.
[16] K. Sato, Y. Achiba, K. Kimura, J. Chem. Phys. 80 (1984) 57.
[17] J.R. Appling, M.R. Harbol, R.A. Edgington, A.C. Goren, J. Chem. Phys. 97 (1992) 4041.
[18] S.N. Dixit, V.C. Mckoy, J. Chem. Phys. 82 (1985) 3546.
[19] T. Suzuki, B.J. Whitaker, Int. Rev. Phys. Chem. 20 (2001) 313.
[20] J.R. Appling, M.G. White, W.J. Kessler, R. Fernandez, E.D. Poliakoff, J. Chem. Phys. 88 (1988) 2300.